

# A low amplitude noise laser for the AURIGA detector optical readout

Livia Conti\*

*Dipartimento di Fisica, Università di Trento and INFN Gruppo coll. Trento, Sez. Padova,  
I-38050 Povo (Trento), Italy*

Maurizio De Rosa, Francesco Marin

*Dipartimento di Fisica, Università di Firenze and INFN Sez. Firenze and LENS, Largo E. Fermi  
2, I-50125 Firenze, Italy*

## Abstract

We have implemented a laser system to be used in an optical transduction chain for the gravitational wave bar detector AURIGA. This system is based on a Nd:YAG laser and includes: quantum limited power stabilization in the acoustic range; deep phase modulation and near quantum limited rf detection for locking to optical cavities; coupling to a single-mode polarization maintaining optical fiber without deteriorating these performances. Such a system has wider applications in optical metrology.

OCSI code: 120.3930, 230.0230, 280.3420.

---

\*Present address: Dipartimento di Fisica, Università di Padova and INFN Sez. Padova, Via Marzolo 8, I-35100 Padova (Italy)

## 1. Introduction

Ultracryogenic resonant detectors of gravitational waves have reached a very high peak spectral sensitivity, thanks to the extremely low level of thermal noise [1]. In order to further increase the burst sensitivity and fully exploit the detector capabilities an improved transduction chain must be implemented for translating the weak bar excitation into a readable signal with the smallest added wideband noise.

In the past an optical signal extraction chain was proposed [2, 3] and partially implemented [4] by J.-P. Richard. The basic idea is to build an optical Fabry-Perot cavity formed by a mirror attached to the bar end face and a second mirror attached to a resonant mechanical transducer (in our case, a central load on a circular elastic plate). The relative motion of the two mirrors is then converted into a frequency shift of the cavity optical resonance frequency.

In the last few years significant technical improvements have much extended the possibilities of frequency references based on stable optical cavities. For example Seel *et. al.* demonstrated the higher level of stability for the integration period between 1 and 100 s. [5]

In the framework of the AURIGA collaboration [6] we are developing a full optical readout for an ultracryogenic resonant bar detector. The AURIGA detector is based on a 3 m long, 0.6 m diameter cylinder, with a mass of 2300 Kg, made with Al5056, an alloy which permits to obtain a high mechanical quality factor  $Q$  at low temperatures. The bar is cooled down to about 0.1 K, where it is characterized by a vibration frequency (first longitudinal mode) of 920 Hz with a  $Q$  of several millions. The scheme of our transduction chain is based on the use of two Fabry-Perot cavities, which we call transducer and reference cavity. [7] The former is installed on a bar end face and its entrance mirror is mounted on a second mechanical resonator with a mass of about 10 Kg. The latter is kept in an acoustically isolated and thermally stabilized (in the range 20-100 °C) environment and, by changing the temperature, it can be tuned with respect to the transducer cavity. A Nd:YAG laser is frequency locked to the transducer cavity by means of a FM sidebands technique [8, 9] and

its frequency fluctuations are monitored using the same technique with the reference cavity. A single-mode polarization maintaining optical fiber is used to carry the laser radiation into the bar vacuum chamber. The beam reflected by the transducer cavity, after an optical circulator, is collected by a second fiber and detected outside the bar chamber.

An efficient implementation of the transduction chain requires a laser system with some special characteristics. In this work we present and discuss the implementation of such a system. In particular, a high laser intensity stability is necessary in the kHz region and the phase sensitive detection must be performed with the highest obtainable sensitivity, i.e., with optimal phase modulation depth and shot-noise limited detection. Moreover, these characteristics must be conserved after the optical fiber transmission.

Even if our system is particularly designed for the use in the optical transduction chain, the results we have obtained are of more general interest and can be easily extended in order to satisfy the requirements of other metrological laser systems.

## 2. System requirements

The transduction chain includes a 1 cm long transducer cavity, with Finesse  $3 \cdot 10^5$ , corresponding to the best commercially available mirror quality. With a detected power of 1 mW and an optimal phase modulation depth (about 1 rad) a shot-noise limited detection yields a residual frequency noise of the laser locked to the cavity (with respect to the cavity itself) of  $2 \cdot 10^{-4} \text{ Hz}/\sqrt{\text{Hz}}$ .

We use the expression *detected power* for the power impinging on the detector times the detector quantum efficiency: the detector is modeled as a beam-splitter with transmission equal to the quantum efficiency, followed by a perfect detector.

Considering the losses in the coupling of the radiation reflected by the transducer cavity into the output fiber (expected around 20%) and the detector quantum efficiency, a laser power of about 2 mW or less must be coupled to the transducer cavity. With these figures and mirror losses (absorption and scattering) of 1 ppm, the laser power dissipated by the

cavity is expected to be few hundreds of  $\mu\text{W}$ , still lower than the AURIGA refrigerator cooling power (about 1.4 mW at 0.1 K). A higher power level would improve the sensitivity, but it can hardly be tolerated by the ultra-cryogenic cooling system.

We will operate in coincidence two independent reference cavities, in order to reduce the possibility of spurious events. The reference cavities detection system should allow a sensitivity better than the one of the transducer cavity, in order to maintain the above calculated performance. Such a result will be obtained with 20 cm long cavities with Finesse around  $4 \cdot 10^4$  and a detected power of 10 mW.

The frequency of the FM sidebands must be large enough to operate in the spectral region where the laser amplitude noise is nearly shot-noise limited. On the other hand, the need to detect a power of at least 10 mW implies the use of relatively large photodiodes, thus limiting the detection bandwidth. As a compromise, the modulation frequency is chosen between 10 and 15 MHz. The frequency modulation and the detection are discussed in detail in Section 4.

A further parameter to be considered is the laser amplitude noise spectrum around 1 kHz. The fluctuations of the laser intensity in the transducer cavity are transformed into mechanical noise by the radiation pressure effect on the cavity mirrors and must be considered as a source of force noise, whose power spectrum  $S_{\text{BA}}$  is:

$$S_{\text{BA}} = \frac{4}{c^2} S_{P_c}, \quad (1)$$

where  $S_{P_c}$  is the intracavity laser amplitude noise power spectrum which can be written as

$$S_{P_c} = S_{P_{\text{in}}} \left( \frac{P_c}{P_{\text{in}}} \right)^2. \quad (2)$$

Here  $S_{P_{\text{in}}}$  is the noise spectrum and  $P_{\text{in}}$  the power of the laser beam entering the cavity, corresponding to about half of the beam impinging on the cavity for the optimal modulation depth.  $P_c$  is the intracavity laser power, given by

$$P_c = P_{\text{in}} T_1 \left( \frac{F}{\pi} \right)^2, \quad (3)$$

where  $T_1$  is the input mirror transmissivity and  $F$  is the cavity Finesse. In order to reduce the effect of the radiation pressure we have to implement an active intensity noise reduction, described in Section 5. With the parameters of Table 1, a shot-noise limited input beam yields a force noise spectral density of  $S_{\text{BA}} = 1.6 \cdot 10^{-28} \text{ N}^2/\text{Hz}$ , nearly two orders of magnitude lower than the calculated thermal noise. We remark that the fluctuations due to the radiation pressure are seen as narrow-band noise at the output of the transduction chain. They can be considered as a back-action effect and they would determine the ultimate sensitivity limit if one could increase the laser power without the present technical limitations.

### 3. Experimental apparatus

A scheme of our system is reported in Fig. 1. The laser source is a 100 mW Nd:YAG (Lightwave 126-1064-100) with internal amplitude stabilization. A -40 dB optical isolator is used to prevent scattering of light into the laser and to obtain a well defined polarization.

An aluminum box contains a first electro-optic modulator (EOM1), a polarizer and a second electro-optic modulator (EOM2). The box is slightly heated (between 30°C and 35°C) up to a selected temperature and thermally stabilized with residual fluctuations of about 0.04°C in 24 hours. The EOM1 is a Gsänger LM0202, with a 5 mm wide crystal and a half-wave voltage  $V_\pi$  of about 560 V at 1064 nm. The EOM2 is a New Focus 4003 resonant modulator. A modulation depth of about 1 rad is obtained by applying an rf power of 20 dBm at the resonant frequency of 13.3 MHz.

After the box a polarizer is followed by a 50% beam-splitter (BS1). The BS1 is replaced by a variable beam-splitter (i.e. an half-wave plate followed by a polarizing beam-splitter) for the measurements described in Section 5. The beam transmitted by the BS1 is detected by a photodiode (PD1). The signal is then amplified and filtered by the loop electronics and sent to the EOM1.

Part of the beam transmitted by the BS1 is coupled into a single-mode polarization

maintaining optical fiber, with integrated lenses at both ends. The overall coupling efficiency is 65%. The beam analysis is performed both before and after the fiber, by means of photodiodes followed by an rf spectrum analyzer or a digital scope with internal FFT data analysis (LeCroy LT342).

For the low-frequency analysis, the calibration of the shot-noise is performed by using a balanced self-homodyne detection. [10] The laser beam is precisely divided into two parts of equal intensity by means of a beam-splitter formed by a half-wave plate and a polarizing beam-splitter. The two outputs of the beam-splitter are sent to separate photodiodes (PD2 and PD3) whose ac signals are amplified and sent to a passive  $+/-$  power combiner. The difference signal gives an accurate calibration of the shot noise of the beam impinging on the beam-splitter, while the sum corresponds to the laser amplitude noise. The calibration has been checked using an halogen light source.

For the rf analysis, a single photodiode (PD4) is used and a shot-noise calibration signal is provided by the thermal light source. The rf signal from PD4 is demodulated in a double-balanced mixer whose IF output is analyzed, after a low-pass filter and an amplifier, using the digital scope. The modulation signal for EOM2 and the local oscillator for the mixer are provided by two phase-locked signal generators (HP 33120A).

#### **4. Phase modulation**

We analyze the laser amplitude noise spectrum at rf frequencies by means of a 2 mm diameter PIN photodiode (EG&G C30642) with a load resistor of 150  $\Omega$  followed by an ac-coupled (frequency  $> 1$  MHz) home-made amplifier. The quantum efficiency of the photodiodes we have used is about 0.9.

The linearity of the photocurrent response versus laser power is within 1% below 20 mW, as checked with a power meter.

In Fig. 2 we show the recorded amplitude noise spectrum of the laser, for a power of 9 mW impinging on the detector. The noise approaches the shot-noise for frequencies higher than

a few MHz. The electronic noise corresponds to the shot-noise level for a power of 3.5 mW on the detector. It is thus negligible for a power larger enough than this value.

We report in Fig. 3 the measured noise power density at 10 MHz for different values of the photocurrent, for both the laser and the white light. The linearity of the latter curve demonstrates that the rf response of the photodiode is linear (up to 20 mA, corresponding to a detected power of about 25 mW). The curve of the laser amplitude noise has a quadratic behaviour:

$$S_L = D + aI + bI^2, \quad (4)$$

where  $S_L$  is the detected noise power density,  $I$  is the photocurrent and, on the right side of Eq. (4), the first term is the electronic noise, the second term is the shot-noise, the third term is the excess noise. The fit of the experimental curve with Eq. (4) gives an excess noise of  $a/b = 75 I$  (A).

At our detection frequency (13.3 MHz), for a power of 11 mW impinging on the detector (10 mW detected power, the value used for the calculation of the system sensitivity in Section 2) the total noise power density is 1 dB above the shot-noise level.

The phase modulation introduces a residual amplitude modulation (RAM) due to laser amplitude modulation by the EOM2, polarization modulation transformed into amplitude modulation by the polarizer, and interference of scattered and reflected light with the main beam (etalon effects). The dc offset produced by the RAM after phase sensitive detection gives rise to a displacement of the locking point from the real line center. The offset we have measured is lower than 0.3% of the peak-to-peak signal amplitude, giving a frequency shift of less than 50 Hz.

What is more important, the fluctuations of the RAM signal must have a negligible spectral power around 1 kHz to avoid decreasing the sensitivity. In Fig. 4 we report the spectrum of the demodulated signal, after the mixer. This spectrum is compared with the one without modulation: the RAM introduces no excess noise around 1 kHz, while it is effective at lower frequencies. The situation is worse after a 12 m long fiber. In that case

(due to interference effects in the fiber) we have measured a noise power at 1 kHz about 9 dB higher than the quantum level, for a laser power of 5 mW. For 1 mW detected power we deduce an excess noise of 2 dB, leading to a 30% decrease in sensitivity.

## 5. Amplitude stabilization

The photodetectors used for the 1 kHz amplitude noise reduction and measurement are the same described in the previous section, with a load resistor of 240  $\Omega$ . The laser power is controlled by means of EOM1 and the following polarizer Pol1. The polarization axis of the laser at the entrance of the EOM1 is rotated by an angle  $\alpha$  of about 0.12 rad with respect to one axe of the EOM1. The polarizer is oriented along the input polarization direction.

The EOM changes the input polarization into elliptical, thus reducing the transmitted power  $P$  according to:

$$P = P_0 \left( 1 - \sin^2 2\alpha \sin^2 \frac{\phi}{2} \right), \quad (5)$$

where  $\phi$  is the phase retardation difference between the two EOM axes. In order to work in a linear response region, we set the temperature of the EOM for an offset phase ( $\phi_0 \sim \pi/2$ ) in one of the EOM axis with respect to the other one, i.e., we work around a slightly elliptical polarization (giving an average transmission of 92%). This phase is then changed by the voltage applied to the EOM in order to correct the laser power fluctuations.

The temperature of the EOM is actively stabilized within 0.04°C, in order to reduce the fluctuations of  $\phi_0$  to less than 0.04 rad. The laser relative amplitude changes induced by the EOM and polarizer system, for a small applied voltage  $\Delta V$ , are:

$$G_{\text{EOM}} = \frac{1}{2} \frac{\pi \Delta V}{V_\pi} \sin^2 2\alpha \sin \phi_0. \quad (6)$$

The photodiode signal is amplified (with a band-pass filter between 500 Hz and 2 kHz) and sent to the EOM. We can define an electronic gain as

$$G_{\text{el}} = G_{\text{pd}} G_{\text{loop}} G_{\text{EOM}}, \quad (7)$$



where  $G_{\text{pd}}$  is the photodetector gain (in V/W) and  $G_{\text{loop}}$  is the loop amplifier transfer function, and a total loop gain

$$G_{\text{tot}} = T G_{\text{el}}, \quad (8)$$

where  $T = 1 - R$ , and  $R$  is the reflectivity of the beam-splitter BS1.

The calculation of the obtainable noise reduction requires a quantum mechanical approach which takes into account the vacuum fluctuations introduced by the beam-splitter. It is shown by Giacobino *et al.* [11] that the noise spectrum of the transmitted beam, normalized to its own shot-noise, is

$$\frac{S_0 R}{(1 + T G_{\text{el}})^2} + \frac{T(1 + G_{\text{el}})^2}{(1 + T G_{\text{el}})^2}, \quad (9)$$

where  $S_0$  is the input noise spectrum normalized to shot noise. For high  $T$  the output noise approaches the shot-noise level, at the expense of a lower transmitted power. In the limit of infinite gain, the output noise spectrum reduces to  $1/T$ .

We have measured the output noise versus BS1 transmissivity, keeping constant the total loop gain  $G_{\text{tot}} = 15$ . Indeed, for a fixed loop frequency response,  $G_{\text{tot}}$  is limited by stability requirements. The results are reported in Fig. 5, together with the theoretical prediction of Eq. (9). The input noise was measured independently, giving  $S_0 = 500$ . The thick line gives the theoretical limit with infinite gain.

In our transduction chain we will use a 50% beam-splitter for BS1, yielding an amplitude noise 5 dB above the quantum level in the transmitted beam, around 1 kHz, with the present active stabilization. In Fig. 6 we show the amplitude noise spectrum in this configuration. The laser power is 30 mW, giving a relative intensity noise of  $-164$  dB/Hz.

The coupling to the optical fiber deteriorates the laser amplitude stability, above all at low frequencies, probably due to mechanical noise in the coupling system. In Fig. 7 we report the noise spectrum measured after a 2 m long fiber for both free-running and actively stabilized laser, compared with the shot-noise. The measurement is performed with a detected power of 15 mW and gives an excess noise, after stabilization, of 7 dB at 1 kHz.

For a laser power of 2 mW or less (the planned laser power at the input of the transducer cavity) the excess noise reduces to less than 2 dB, corresponding to amplitude fluctuations lower than  $1.2 \cdot 10^{-21}$  mW<sup>2</sup>/Hz. The back-action, according to Eqs. (1) and (2), will be less than  $2 \cdot 10^{-28}$  N<sup>2</sup>/Hz, i.e., 50 times lower than the transducer thermal noise.

## 6. Conclusions

We have implemented a laser system with the following characteristics.

The beam is phase-modulated at 13.3 MHz, with a modulation depth of about 1 rad. The RAM is below 0.3%. The noise power of the detected and demodulated signal, around 1 kHz, is 1 dB above the shot-noise level for 10 mW detected power and 2 dB for 1 mW detected power after a 12 m single-mode polarization maintaining optical fiber.

The intensity is stabilized around 1 kHz, with a residual excess noise of 5 dB for 30 mW laser power and 2 dB for 2 mW laser power after the fiber.

Such a system, when used in a transduction chain like the one described by Conti *et al.* in Ref. 7 (see also Sec. 1), would allow the AURIGA detector to reach a burst sensitivity of  $2 \cdot 10^{-20}$  with a bandwidth of 80 Hz. These results are the first step towards the realization of a prototype of optical transduction chain for gravitational wave resonant detectors.

The characteristics of our laser system compare well with the fundamental limits given by the quantum theory. Even if this work is particularly focused on the AURIGA optical readout, the results here reported are of wider interest in the field of high performance metrological laser systems.

## Acknowledgements

We want to thank the AURIGA collaboration, in particular M. Cerdonio, G.A. Prodi, L. Taffarello, S. Vitale, and J.-P. Zendri. We also thank M. Inguscio and the LENS staff.

Correspondence should be addressed to Francesco Marin ([marin@lens.unifi.it](mailto:marin@lens.unifi.it)).

## REFERENCES

1. M. Cerdonio, L. Baggio, V. Crivelli Visconti, L. Taffarello, J. P. Zendri, G. A. Prodi, L. Conti, R. Mezzena, S. Vitale, M. Bonaldi, P. Falferi, V. Martinucci, A. Ortolan, G. Vedovato, and P. L. Fortini, in *Gravitation and Relativity: at the Turn of the Millennium, Proc. of the 15<sup>th</sup> Int. Conf. on General Relativity and Gravitation*, edited by N.Dadhich and J.Narlikar, IUCAA (Inter-University Centre for Astronomy and Astrophysics), Pune (India) (1998).
2. J.-P. Richard, “Laser instrumentation for one-phonon sensitivity and wide bandwidth with multimode gravitational radiation detectors”, *J. Appl. Phys.* **64**, 2202-2205 (1988).
3. J.-P. Richard, “Approaching the quantum limit with optically instrumented multimode gravitational-wave bar detectors”, *Phys. Rev. D* **64**, 2309-2317 (1992).
4. Y. Pang and J.-P. Richard, “Room temperature tests of an optical transducer for resonant gravitational wave detectors”, *Appl. Opt.* **34**, 4982-4988 (1995).
5. S. Seel, R. Storz, G. Ruoso, J. Mlynek, and S. Schiller, “Cryogenic Optical Resonator: A New Tool for Laser Frequency Stabilisation at the 1 Hz Level”, *Phys. rev. Lett.* **78**, 4741-4744 (1997).
6. M. Cerdonio, M. Bonaldi, D. Carlesso, E. Cavallini, S. Caruso, A. Colombo, P. Falferi, G. Fontana, P. L. Fortini, R. Mezzena, A. Ortolan, G. A. Prodi, L. Taffarello, G. Vedovato, S. Vitale, and J. P. Zendri, “The ultracryogenic gravitational-wave detector AURIGA”, *Cl. Quant. Grav.* **14**, 1491-1494 (1997); G. A. Prodi, L. Conti, R. Mezzena, S. Vitale, L. Taffarello, J. P. Zendri, L. Baggio, M. Cerdonio, A. Colombo, V. Crivelli Visconti, R. Macchietto, P. Falferi, M. Bonaldi, A. Ortolan, G. Vedovato, E. Cavallini, and P. Fortini, “Initial Operation of the Gravitational Wave Detector AURIGA”, in *Proc. Of the 2nd E. Amaldi Conf. On Grav. Waves*, p. 148-158, edited by E. Coccia, G. Pizzella and G. Veneziano (World Scientific, Singapore, 1998).

7. L. Conti, M. Cerdonio, L. Taffarelo, J.P. Zendri, A. Ortolan, C. Rizzo, G. Ruoso, G.A. Prodi, S. Vitale, G. Cantatore, and E. Zavattini, "Optical transduction chain for gravitational wave bar detectors", *Rev. Sci. Instrum.* **69**, 554-558 (1998).
8. R.W.P. Drever, J.L. Hall, F.V. Kowalski, J. Hough, G.M. Ford, A. J. Munley, and H. Ward, "Laser phase and frequency stabilization using an optical resonator", *Appl. Phys. B* **31**, 97-105 (1983).
9. D. Hills and J. L. Hall, "Response of a Fabry-Perot cavity to phase modulated light", *Rev. Sci. Instrum.* **58**, 1406-1412 (1987).
10. H. P. Yuen, V. W. S. Chan, "Noise in homodyne and heterodyne detection", *Optics Lett.* **8**, 177-179 (1983).
11. E. Giacobino, F. Marin, A. Bramati and V. Jost, "Quantum noise reduction in lasers", *J. Nonlin. Opt. Phys. Mat.* **5** 863-877 (1996).

## List of Figures

1	Experimental setup. $\lambda/2$ : half-wave plate; EOM: electro-optic modulator; Pol: polarizer; BS: beam-splitter; PD: photodiode. . . . .	16
2	Upper curve: intensity noise power, for 9 mW impinging on the detector. Middle curve: shot-noise calibration obtained with an halogen lamp. Lower curve: detector electronic noise. . . . .	17
3	(a) Power spectral density at 10 MHz of the intensity noise as a function of the photocurrent generated by an halogen lamp (lower curve, fitted with a straight line) and by the laser (upper curve, fitted with a 2nd order polynomial). P1, P2, P3 are, respectively, the coefficients of the 0th, 1st, 2nd order terms in the fitting function. b) Laser power density normalized to shot noise as a function of the photocurrent. Percentage deviations from the fitting curves are shown on the bottom, respectively (c) for the halogen lamp, (d) the laser and (e) the noise ratio. . . . .	18
4	Intensity noise spectrum measured after detection at 13.3 MHz and demodulation in a double-balanced mixer. Upper curve: phase modulated laser. Middle curve: without modulation. Lower curve: electronic noise. . . . .	19
5	Intensity noise spectral density, referred to shot noise, as a function of the transmissivity of the beam-splitter BS1. The experimental data a fitted with Eq. (9). The thick curve represents the theoretical limit for infinite gain. . .	20
6	Intensity noise spectra in the acoustic range, taken with the balanced detection for 30 mW laser power. Upper curve: laser noise (balanced detection in the sum position) without active stabilization. Middle curve: the same, with the stabilization loop on. Lower curve: shot-noise reference, measured with the balanced detection in the difference position. . . . .	21
7	The same spectra as in Fig. 6, measured after the optical fiber for 15 mW laser power. . . . .	22

## TABLES

Table 1. Parameters used for the calculations reported in the text.

---

Reference cavity Finesse	$4 \cdot 10^4$
Transducer cavity Finesse	$3 \cdot 10^5$
Transducer cavity input mirror transmission	10 ppm
Phase modulation depth	1 rad
Laser power impinging on the transducer	2 mW
Detected power for the transducer cavity photodiode	1 mW
Detected power for the reference cavity photodiode	10 mW
Transducer thermal noise	$10^{-26} \text{ N}^2/\text{Hz}$

---

# FIGURES

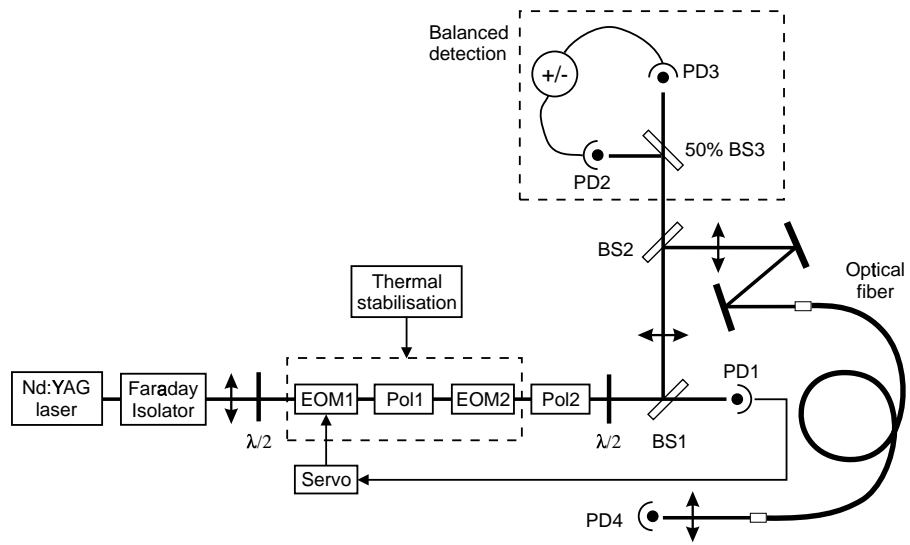


Fig. 1. Experimental setup.  $\lambda/2$ : half-wave plate; EOM: electro-optic modulator; Pol: polarizer; BS: beam-splitter; PD: photodiode.



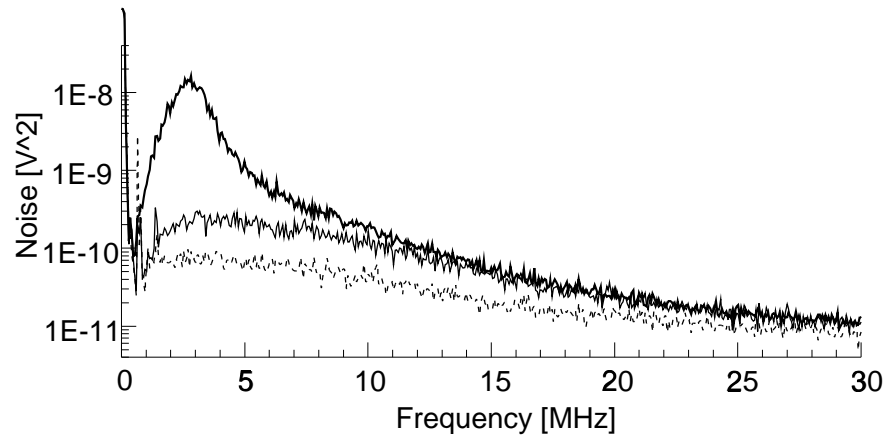


Fig. 2. Upper curve: intensity noise power, for 9 mW impinging on the detector. Middle curve: shot-noise calibration obtained with an halogen lamp. Lower curve: detector electronic noise.

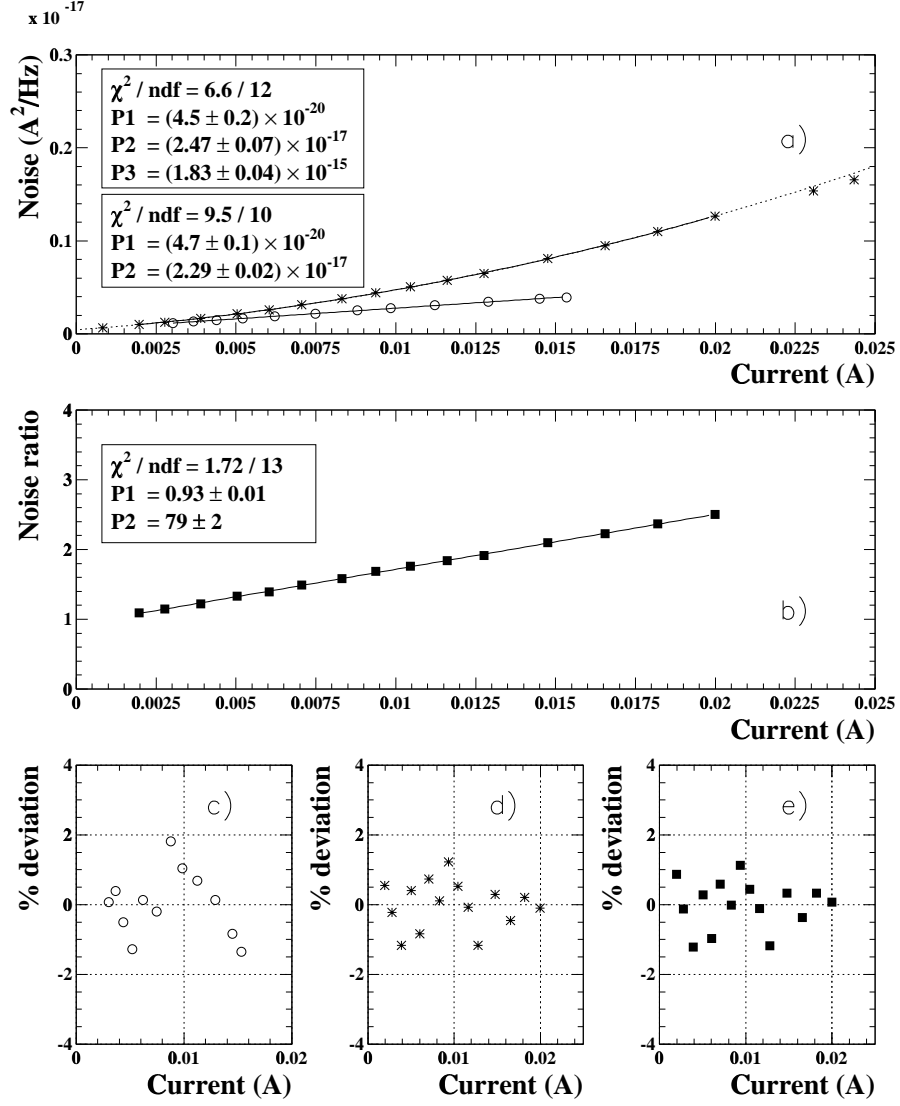


Fig. 3. (a) Power spectral density at 10 MHz of the intensity noise as a function of the photocurrent generated by an halogen lamp (lower curve, fitted with a straight line) and by the laser (upper curve, fitted with a 2nd order polynomial). P1, P2, P3 are, respectively, the coefficients of the 0th, 1st, 2nd order terms in the fitting function. b) Laser power density normalized to shot noise as a function of the photocurrent. Percentage deviations from the fitting curves are shown on the bottom, respectively (c) for the halogen lamp, (d) the laser and (e) the noise ratio.

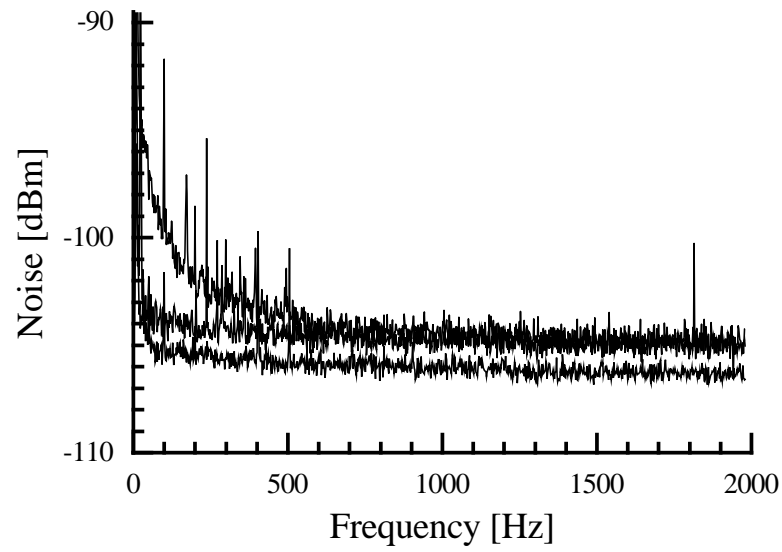


Fig. 4. Intensity noise spectrum measured after detection at 13.3 MHz and demodulation in a double-balanced mixer. Upper curve: phase modulated laser. Middle curve: without modulation. Lower curve: electronic noise.

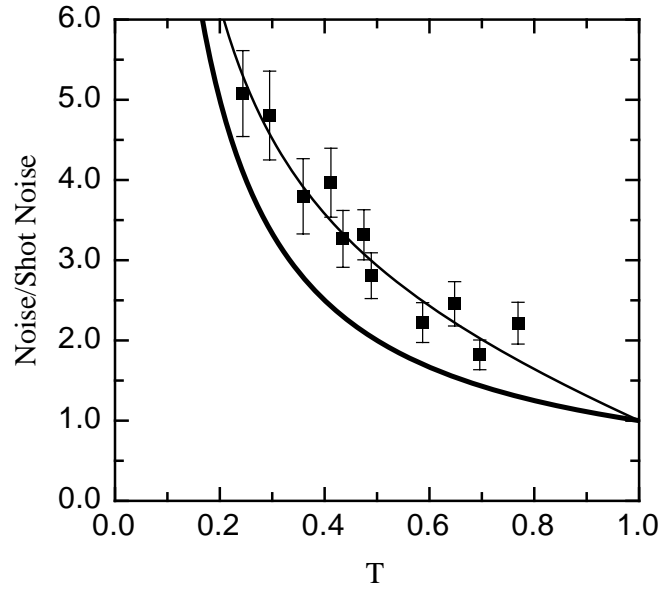


Fig. 5. Intensity noise spectral density, referred to shot noise, as a function of the transmissivity of the beam-splitter BS1. The experimental data are fitted with Eq. (9). The thick curve represents the theoretical limit for infinite gain.

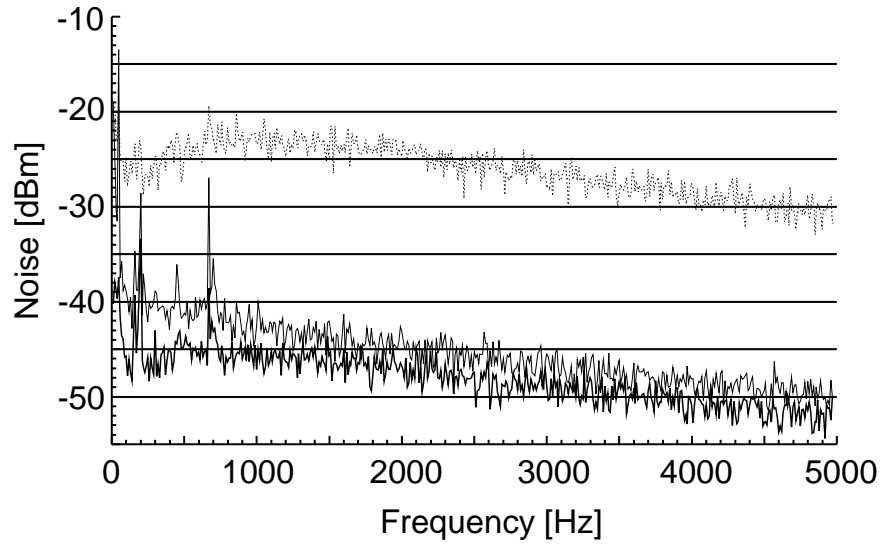


Fig. 6. Intensity noise spectra in the acoustic range, taken with the balanced detection for 30 mW laser power. Upper curve: laser noise (balanced detection in the sum position) without active stabilization. Middle curve: the same, with the stabilization loop on. Lower curve: shot-noise reference, measured with the balanced detection in the difference position.

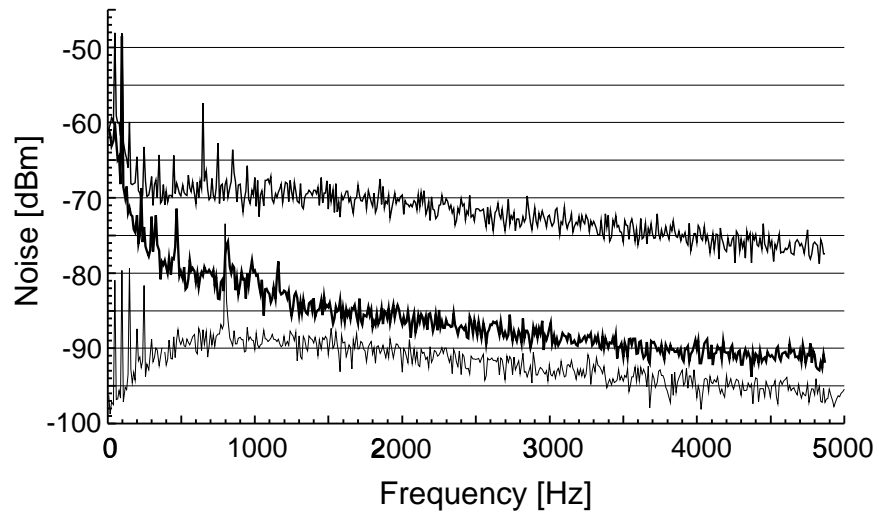


Fig. 7. The same spectra as in Fig. 6, measured after the optical fiber for 15 mW laser power.